

Journal of Natural Fibers



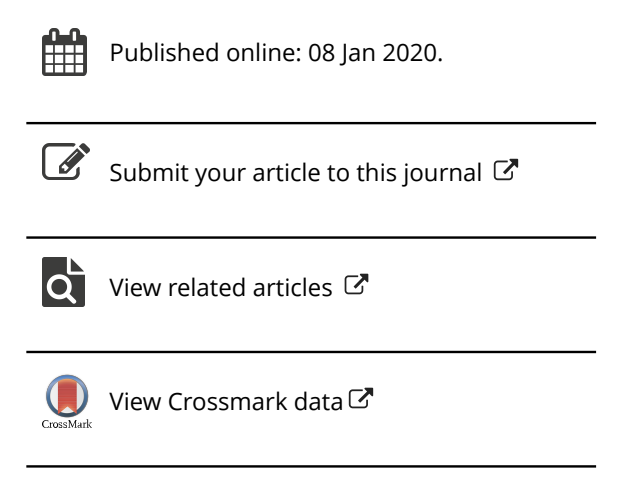
ISSN: 1544-0478 (Print) 1544-046X (Online) Journal homepage: https://www.tandfonline.com/loi/wjnf20

Effect of Sodium Hydroxide Treatment on Physico-chemical, Thermal, Tensile and Surface Morphological Properties of *Pongamia Pinnata L*. Bark Fiber

M. Umashankaran & S. Gopalakrishnan

To cite this article: M. Umashankaran & S. Gopalakrishnan (2020): Effect of Sodium Hydroxide Treatment on Physico-chemical, Thermal, Tensile and Surface Morphological Properties of *Pongamia Pinnata L.* Bark Fiber, Journal of Natural Fibers, DOI: 10.1080/15440478.2019.1711287

To link to this article: https://doi.org/10.1080/15440478.2019.1711287







Effect of Sodium Hydroxide Treatment on Physico-chemical, Thermal, Tensile and Surface Morphological Properties of *Pongamia Pinnata L.* Bark Fiber

M. Umashankaran^a and S. Gopalakrishnan^b

^aDepartment of Mechanical Engineering, N.S.N. College of Engineering and Technology, Karur, India; ^bDepartment of Mechanical Engineering, K.S. Rangasamy College of Technology, Tiruchengode, India

ABSTRACT

Surfaces of Pongamia pinnata L. fiber (PPF) were modified by the 5% (w/v) sodium hydroxide solution with the various immersing period as 15, 30, 45, 60 and 75 minutes. Chemical compositional analysis evidenced that 5% (w/ v) sodium hydroxide solution with 60 minute immersing period is optimum treatment. Removal of lignin content from the optimally treated PPF was detected through the chemical analysis as well as Fourier Transform-Infrared spectroscopy. X-ray diffraction analysis outcomes established the enhancement in the crystallinity index (45.31% to 52.43%) and crystallite size (5.43 nm to 8.32 nm) of the optimally surface-modified PPF. Improvement in the maximum cellulose degradation temperature (332°C to 348°C) and kinetic activation energy of the optimally-surface modified fibers (68.642 KJ/mol to 72.563 KJ/mol) were acknowledged from differential thermogravimetric curve and broido plots. Scanning electron microscope and atomic force microscopy investigations visualized the improvement in surface roughness of the PPF after alkalization. All the above findings authorized the suitability of optimally surface modified PPF as reinforcement in lightweight polymer composite applications.

摘要

Pongamia pinnata L. 纤维 (PPF) 的表面由 5% (w/v) 氢氧化钠溶液进行改性,各种浸浸期为 15、30、45、60 和 75 分钟. 化学成分分析表明,5% (w/v) 氢氧化钠溶液具有60分钟的浸泡期是最佳处理. 通过化学分析和傅立叶变换红外光谱法,从最佳处理的PPF中去除木质素含量. X射线衍射分析结果证实结晶度指数的增强(45.31%至52.43%)和最佳表面改性PPF的结晶尺寸(5.43 nm 到 8.32 nm). 从差分热重力曲线和溴多图中确认最佳表面改性纤维(68.642 KJ/mol 至 72.563 KJ/mol)的最大纤维素降解温度(332℃至 348℃)和动能活化能量的改善. 扫描电子显微镜和原子力显微镜研究可视化了碱化后PPF表面粗糙度的改善. 上述所有发现都认可了最佳表面改性PPF作为轻质聚合物复合材料应用的增强物的适用性.

KEYWORDS

Pongamia pinnata L. fiber (PPF); alkali treatment; optimally surface-modified fibers; chemical analysis and thermal stability

关键词

纤维(PPF); 碱处理; 最 佳表面改性纤维; 化学分 析和热稳定性

Introduction

Today, natural fiber reinforced plastic materials are getting higher demand due to their low cost, easy fabrication procedures, corrosion resistance and higher availability of natural fibers (Thakur and Thakur 2014). Addition to this, many of the countries have banned the usage of non-biodegradable synthetic fiber reinforced composites to prevent the environment from pollutions which increase the demand for the natural fiber reinforced composites day by day (Liu et al. 2019b). Currently,

automobile and related industries are fabricating the composite materials by using commercially available plant fibers such as jute, hemp, flax and sisal. However, it is difficult to satisfy the current market demand for plant fiber by using commercially available plant fibers alone. So that, many of the researchers are searching the new natural fibers to replace the synthetic fibers (Sanjay et al. 2019) Based on the origin, natural fibers are classified into two categories such as plant-based fibers (Cellulosic fibers) and animal-based fibers (protein fibers). Plant fibers are made of different chemical constitutions such as cellulose, hemicellulose, lignin and wax (Manimaran et al. 2018d). Thermal stability and single fiber tensile strength of the plant fibers are majorly based on the amount of cellulose content existing in the fiber. Lignin content in the fiber is preventing the fiber from the biological attacks. Hemi- cellulose and wax content existing in the fiber may reduce the bonding strength between the fiber and matrix while fabricating the composites due to its hydrophilic nature (Madhu et al. 2018a). So, it is mandatory to alter the surfaces of the plant fibers before fabricating the polymer composites. Surfaces of the plant fibers can be modified through either physical modification techniques (Plasma treatment, Laser treatment, y -Ray treatment, corona treatment, etc.) or chemical modification techniques (alkali-treatment, Acetic acid treatment, Silane treatment, etc.) (Sathishkumar et al. 2013). Among them, many of the researchers used sodium hydroxide treatment (alkali-treatment) due to simple handling procedure and effectiveness. However, it is essential to optimize the sodium hydroxide concentration as well as the soaking period. Many of the researchers found that 5 (W/V) % is the optimized concentration at the same time, fiber to fiber, there is a variation in the soaking time (Saravanakumar et al. 2014). In this research article, we optimized the soaking time for the alkali- treatment of the Pongamia pinnata L. bark Fibers by chemical analysis method and studied the impact of surface modification (NaOH treatment) on physical, chemical, thermal, tensile and surface morphological properties of the PPF by Chemical compositional analysis, Fourier Transform-Infrared spectroscopy (FT-IR), X-ray Diffraction Analysis (XRD), Thermal analysis, Single-fiber tensile testing, Scanning Electron Microscope (SEM), Energydispersive X-ray spectroscopy (EDX) and Atomic force microscopy (AFM).

Materials and methods

Materials

Raw Pongamia pinnata L. bark Fibers, NICE brand analytical-grade sodium hydroxide (NaOH) pallets (98% purity), hydrochloric acid (HCL) and Demineralized water (NICE brand) (PH value of 5.5 to 7) were utilized for the analysis.

Fiber extraction

Aged barks of the PP were gathered from Thalapatti village located in Karur district, Tamilnadu, India. Healthy barks were selected and immersed underwater for ten days. After biological retting, separated fiber layers were taken from the water. Separated fiber layers were chopped into small pieces and placed under sunlight for 3 days to eliminate the moisture.

Alkali treatment

Figure 1 illustrated (a) extracted barks of PP plant (b) water retting process (c) extracted raw PPF (d) Sodium hydroxide treatment of PPF. Dried raw fibers were submersed in 5 (W/V) % of aqueous sodium hydroxide solution for 5 various immersing timing (15min, 30min, 45min, 60min and 75min). After immersing periods, fibers were taken from the NaOH solution and kept under diluted hydrochloric acid (0.1N) solution for 2 minutes (Reddy et al. 2013). After that, alkali treated PPFs were several times washed by demineralized water and then dehydrated in a hot oven (80°C) for 6 hours. Dried PPF were preserved in polythene pockets until sending the fiber for further analysis

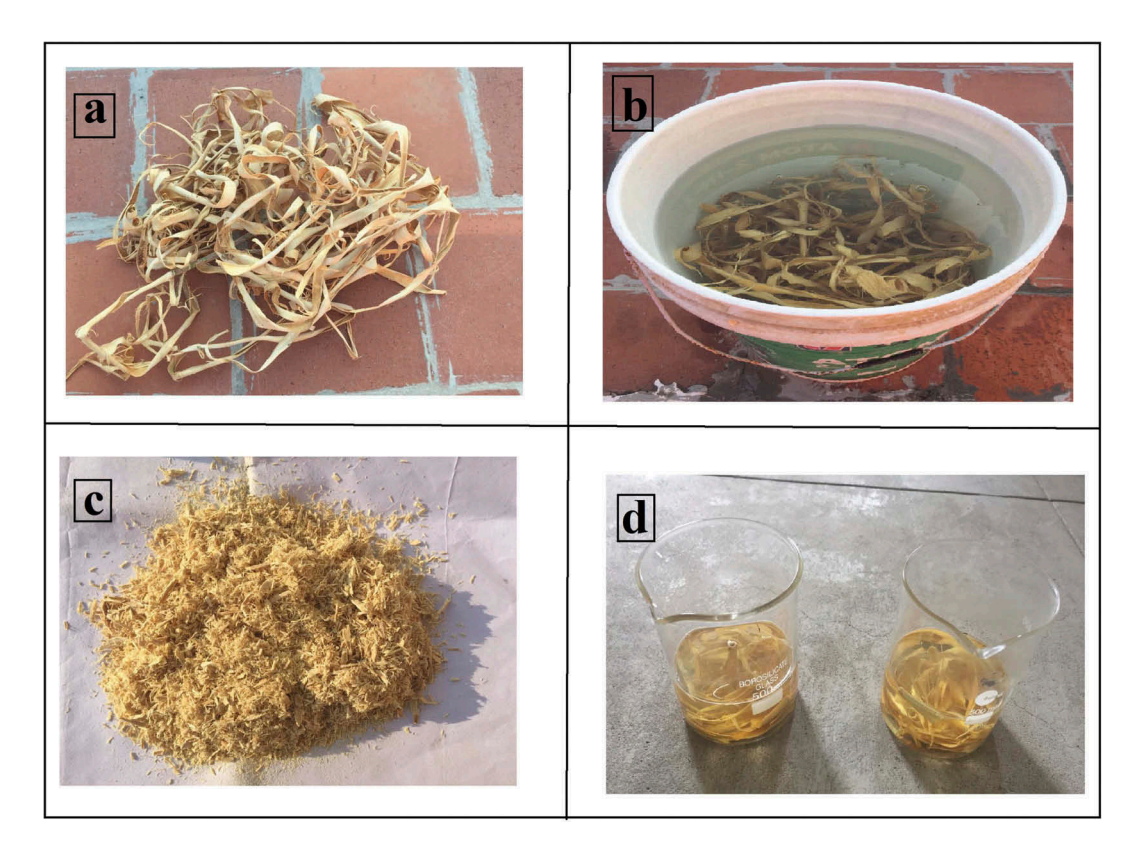


Figure 1. (a) Extracted barks of PP plant (b) Water retting process (c) Extracted raw fiber (d) NaoH treatment of PPF.

Chemical compositional analysis

The quantity of α -cellulose, lignin and ash content exiting in PPF was calculated through the standard practice recommended by the Technical Association of the Pulp and Paper Industry (Reddy et al. 2016). Percentage of Holo- cellulose content in the PPF was estimated through the method designed by the Wise et al. (Reddy et al. 2013). The variation between the α -cellulose and Holo- cellulose was fixed as hemicellulose content. The density of PPF was decided as per the guidelines of ASTM D3800 method (Rwawiire and Tomkova 2015). A textile moisture meter was utilized to finalize the moisture content in the fiber.

Identification of chemical functional groups

Differences in chemical bonds and chemical constitution of the raw and optimally surface-modified PPF were identified through the FTIR (Hyness et al. 2018). This analysis was conducted with the aid of Nicolet iS10 FT-IR spectrometer in the wavenumber span of 4000 to 500 cm⁻¹. Powdered fiber samples were uniformly blended with the potassium permanganate (KBr) in the proportion of 1 (fiber):10 (KBr) and pellets were prepared to run the experiment. Both raw and optimally treated fiber blended pellets were scanned with the resolution of 4 cm⁻¹ and a speed of 2 mm/sec.

Estimation of crystallinity index (CI) and crystallite size (CS)

X-ray diffraction analysis of untreated and optimally surface-modified PPF was conducted to find the improvements in the CI and CS values of optimally treated PPFs. Experiments were run in

Rigaku Ultima IV X-ray diffraction system. Powdered fiber samples were placed on the sample holder, and X-rays were sent through the fibers. Diffracted X-rays were detected from $2\theta = 10^{\circ}$ to 80° . The detector was rotated with 0.02° per step. CI of the untreated and optimally treated PPF were calculated through the mathematical relationship (Equation (1)) (Segal et al. 1959).

$$CI = \left(\frac{I_{002} - I_{am}}{I_{002}}\right) \times 100\% \tag{1}$$

Where, I_{002} altitude of the peaks at 23° and I_{am} altitude of the peaks at 18°. CS values of raw and optimally surface-modified PPF were estimated by the following Equation (2) (Ganapathy et al. 2019).

$$CS_{23} = \frac{0.89\lambda}{\beta_{23}\cos\theta} \tag{2}$$

Where, β_{23} – FWHM (full-width at half-maximum) of the peak at $2\theta = 23^{\circ}$, λ - 1.54178 nm and θ – Bragg angle.

Evaluation of thermal stability and kinetic activation energy (ea)

Chances in the thermal behavior of optimally surface-modified PPF were identified through the TG (thermogravimetric) and DTG (differential thermogravimetric) curves (Shanmugasundaram, Rajendran, and Ramkumar 2018). These analyses were conducted by using a NETZSCH STA 449F3 thermal analyzer. The temperature of the samples was raised from 30°C to 550°C in a nitrogen environment with the rate of heating of 5°C per minute. Mass of the samples was documented for every 1° temperature increment to produce the thermograms.

Surface morphological analyses

Scanning electron microscope (SEM)

The outer layers of the untreated and optimally surface-modified PPF were scrutinized with the aid of a SIGMA HV – Carl Zeiss SEM machine. A gold coating was coated on the surfaces of the raw and optimally surface-modified PPF to convert them as a conductive material.

Energy-dispersive X-ray spectroscopy (EDX)

Energy-dispersive X-ray spectrum was studied to compare the quantity of chemical elements existing on the outer layer of the untreated and optimally-surface modified PPF (Manimaran et al. 2018b). An external attachment in the SEM machine (Z10 EDS Detector) was used for this analysis. This analysis was conducted with an accelerated voltage of 20 kV.

Atomic force microscopy (AFM)

AFM is the precise tool to assess the surface topography of the natural fiber as quantitative values such as average roughness (R_a), Roughness skewness (R_{sk}), Roughness kurtosis (R_{ku}), ten-point average roughness (R_z), Maximum peak-to-valley height (R_t) and Root mean square roughness (R_{q-}) (Saravana Kumaar et al. 2017). A Park XE-70 machine was used to scan the sample in noncontact mode with the frequency, the amplitude of 293.93 \times 10³ HZ and 1.49 μ m respectively. All the images were exported with the resolution 256 pixels.

Single-fiber tensile test

Tensile testing of untreated and optimally surface-modified PPF was executed by using an INSTRON UTM (universal testing machine) with the model number of 5565. ASTM D 3822–07 standard was



followed to calculate the tensile properties (Baskaran et al. 2018). Totally 20 fiber samples with the 50mm length were measured for each case, and average values were tabulated. It is better to analyze the tensile properties of the plant fiber by the statistical method so that Weibull distribution analyzing for tensile strength and modulus were performed by using Minitab 17 software (Senthamaraikannan and Kathiresan 2018).

Results and discussion

Optimally surface-modified fibers

5% (w/v) sodium hydroxide treatment for 60 minutes immense time made the positive modifications in the chemical compositions of PPF when compare to the PPF treated in the other immersing period (15, 30, 45 and 75 minute). Particularly, comparatively elevated (wt. %) cellulose content, lesser hemicellulose and lignin content, as exposed in Table 1. Generally, single fiber tensile strength, thermal stability and kinetic activation energy of the plant fibers were increased when enhancement in the cellulose content so that, 5% (w/v) sodium hydroxide with 60-minute immense time was considered as an optimal surface modification for PPF (Saravanakumar et al. 2014). The chemical compositions of untreated PPF stated in our previous article were taken for the comparison (Umashankaran. and Gopalakrishnan. 2019).

Chemical compositional analysis

The chemical constitutions of bark fibers majorly influence the tensile, structural, thermal and surface topography of the fibers (Indran and Edwin Raj 2015). Cellulose, hemicellulose, lignin, wax are the four primary compositions in plant fiber which is depending on the maturity, soil condition of plant grown, part of the plant which yields the fiber and extraction technique. The alkali treatment converted a small amount of hemicellulose into native cellulose so that, cellulose content of optimally surface-modified PPF was improved to 71.32 Wt. % from 62.34 Wt. % and hemicellulose content were diminished to 7.76 from 14.57 Wt. %. The lignin content of the optimally surface-modified PPF was also lowered (12.54 Wt. % to 6.32 Wt. %) which enabled the single fibers detachment from the fabric. Elimination of the wax and other oily materials are essential for the natural fibers because they are disturbing the bonding strength between the fiber and polymer while fabricating the composites (Liu et al. 2019a). Positively wax content of the optimally surfacemodified PPF was condensed from 0.74 Wt. % to 0.32 Wt. %. The moisture content of the optimally treated PPF also was shortened to 6.68 Wt. % from 12.31 while ash content was elevated to 7.92 Wt. % from 5.46 Wt. %. The density of the optimally surface-modified fiber was slightly raised to

Fiber name	Cellulose (wt.%)	Hemi-celluloses (wt.%)	Lignin (wt.%)	Wax (wt.%)	Moisture Content (%)	Ash(wt.%)	Density (kg/m³)
Raw PPF	62.34	14.57	12.54	0.74	12.31	5.46	1345
5% (w/v) NaoH with 15 min treated PPF	64.53	12.75	10.38	0.64	10.67	6.76	1362
5% (w/v) NaoH with 30 min treated PPF	66.72	10.35	8.96	0.58	9.43	7.12	1374
5% (w/v) NaoH with 45 min treated PPF	68.84	9.04	7.42	0.44	7.64	7.57	1379
5% (w/v) NaoH with 60 min treated PPF	71.32	7.76	6.32	0.32	6.68	7.92	1386
(optimally surface modified PPF)							
5% (w/v) NaoH with 75min treated PPF	68.43	6.34	5.08	0.24	5.68	8.34	1393

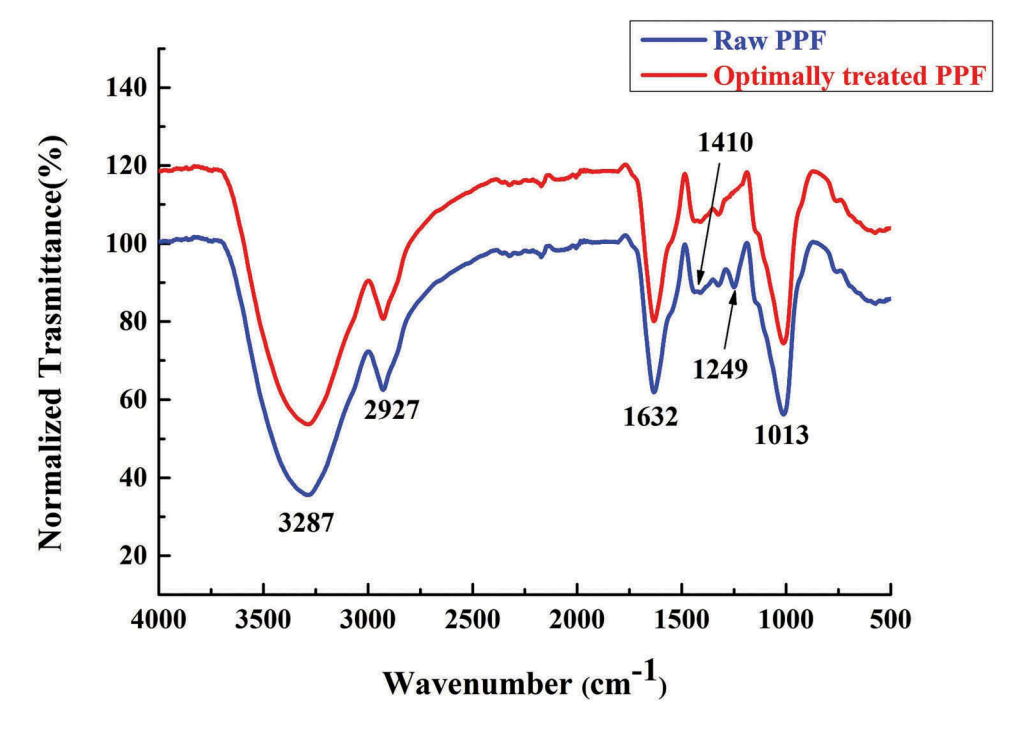


Figure 2. FTIR spectroscopy of the untreated and optimally surface modified PPF.

1386 kg/m³ from 1345 kg/m³. However, it is very lower than the man-made fibers (Arthanarieswaran, Kumaravel, and Saravanakumar 2015). Filling of gaps and cavities in the external surface of the fibers are the reason for a slight rise in density of the alkalized PPF.

Identification of chemical functional groups

FTIR spectroscopy of the raw and optimally surface-modified PPF is displayed in Figure 2. Figure 2 visualizes that raw and optimally surface-modified PPFs have nearly identical FT-IR spectrum; however, there was a small variation spotted on the optimally treated fiber due to the alkalization. Chemical functional groups and related chemical constitution in the untreated and optimally surface-modified PPF were tabularized in Table 2. There are five peaks which are marked at 3287, 2927, 1632, 1410 and 1013 cm-1 on the FTIR spectrum raw and optimally surface-modified PPF. One more additional peak was found in the spectrum of raw PPF at 1249 cm-1 which was pronounced due to existing of lignin content (C = O vibration) (Kılınç et al. 2018a). On the other hand, peak at 1249 cm-1 was missing in the

Table 2. Chemical functional groups and related chemical constitution exiting in the untreated and optimally surface modified PPF.

Peak locations (Wave number (cm-1))		Related chemical Functional group	Related chemical constitution	Reference	
Raw	Optimally treated fiber				
3287	3287	OH vibration	α-Cellulose and Hemi- Cellulose.	(Ali 2016)	
2927	2927	CH vibration	α-Cellulose	(Maheswari et al. 2013)	
1632	1632	C = O stretching	Hemicelluloses	(KılınÇ et al. 2018a)	
1410	1410	CH ₂ vibration	Cellulose	(Atigah et al. 2018)	
1249	-	C = O vibration	Lignin	(Kılınç et al. 2018b)	
1013	1013	C-OH vibration	Lignin	(Manimaran et al. 2018c)	

optimally treated PPF which once again proved the elimination of lignin content from PPF after alkalization. An extended peak at 3287 cm-1 demonstrated the OH vibration of α -cellulose as well as hemicellulose (Ali 2016). A moderate peak at 2927 cm-1 accredited to α -Cellulose (CH vibration) (Maheswari et al. 2013). A sharp peak was detected at 1632 cm-1 designated the C = O vibration of hemicelluloses (KılınÇ et al. 2018b). A little peak was marked at 1410 cm-1 authorized the CH₂ vibration of Cellulose (Atiqah et al. 2018). A "V" shaped peak was highlighted at 1013 cm-1 which is accredited to C-OH vibration arose from Lignin. (Manimaran et al. 2018c).

Estimation of crystallinity index (CI) and crystallite size (CS)

X-ray diffractograms of untreated and optimally surface-modified PPF were exhibited in Figure 3. Generally, natural fibers have two identical peaks around 15° and 22° which are corresponding to the cellulose I (1 1 0) and IV (0 0 2) respectively (Sreenivasan et al. 2011). Another tiny peak existing around 15° designated the amorphous fractions existing in the fiber (Syafri et al. 2018) . Figure 5 clearly revealed that there is a noticeable increase in the intensity of peak at 22° after alkali treatment which confirms the improvement of crystalline fraction in the optimally surface-modified PPF. The CI value of the PPF is improved from 45.31% to 52.43%. The CI of the optimally surface-modified PPF is larger than the *Cissus quadrangularis* stem (47.15%), Napier grass (36.2%), *Juncus effusus L* (33.4%) and *Grewia tilifolia* (8.8%) respectively (Indran and Edwin Raj 2015; Reddy et al. 2009; Maache et al. 2017; Jayaramudu, Guduri, and Varada Rajulu 2010). After the alkali treatment, CS of the optimally surface-modified PPF was enhanced to 8.32 nm from 5.43 nm. The enhancement in crystallite size is a beneficial change because moisture uptaking nature of plant fiber is based on the CS value of the fiber (Reddy et al. 2013).

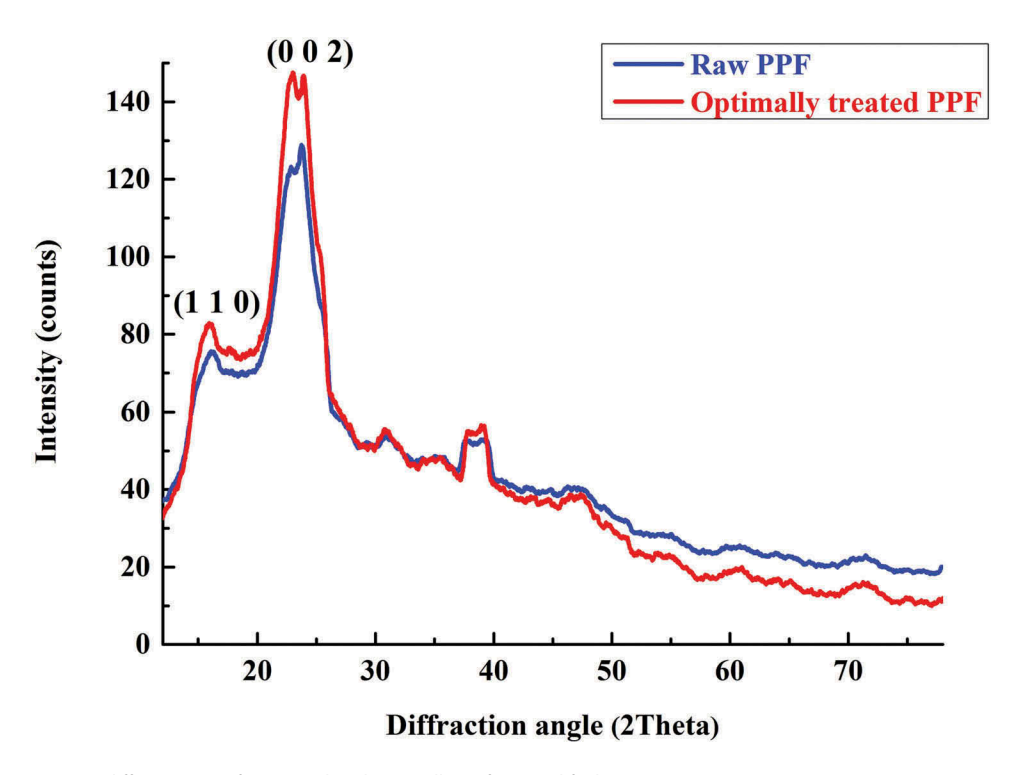


Figure 3. X-Ray diffractogram of untreated and optimally surface modified PPF.



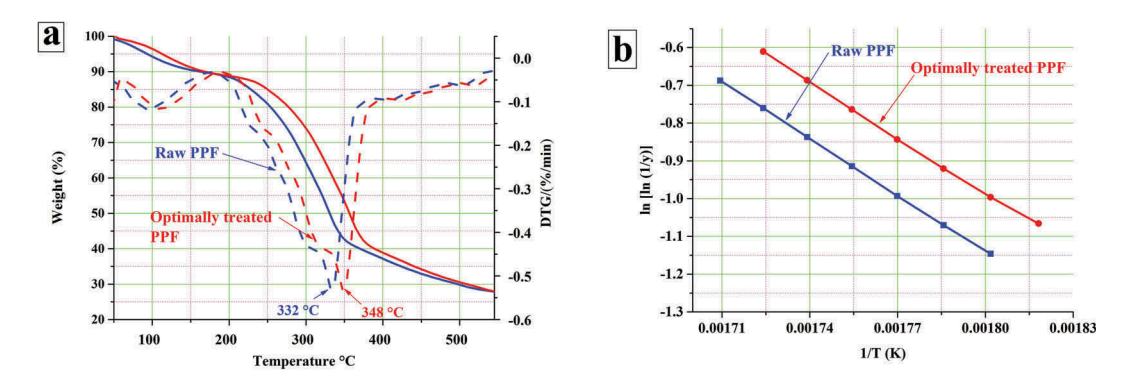


Figure 4. (a) Thermo grams and (b) brido plots of untreated and optimally surface modified PPFs.

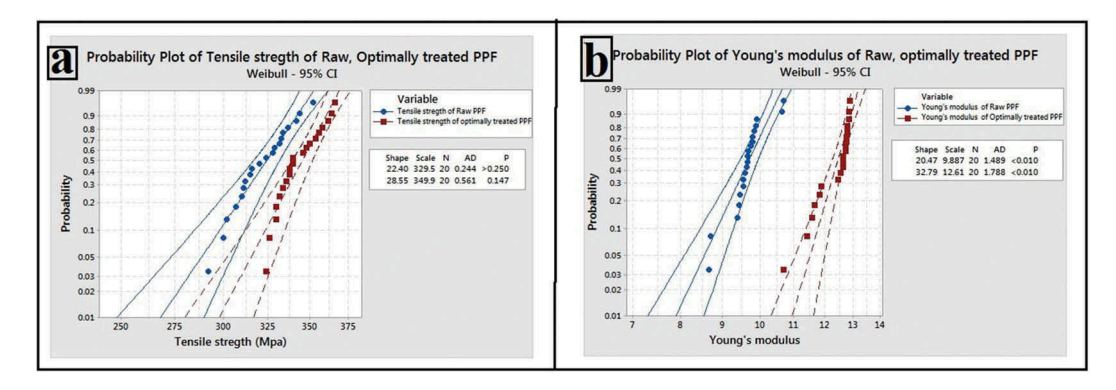


Figure 5. Weibull distribution curves of tensile strength and young's modulus of raw and optimally surface modified PPFs.

Evaluation of thermal stability and kinetic activation energy (E_a)

Usually, higher temperatures are applied to fabricate the natural fiber reinforced thermoplastics so, it is necessary to check the thermal behaviors (thermal stability and Kinetic activation energy) of natural fibers to decide the exact processing temperature of the composites. Thermo grams of untreated and optimally surface-modified PPFs were illustrated in Figure 4a. TG curve demonstrated that untreated and optimally surface-modified fibers have three-stage mass losses. For both the fibers, the first stage of mass loss happened from 30°C to around 210°C which is accredited to the eradication of wetness from the fibers (Kumar et al. 2018). For the raw PPF, the second step of weight damage was observed from 210°C to 360°C. On the other hand, the second phase was noticed from 210°C to 375°C for the optimally surface-modified fiber. The second step of mass loss was related to the simultaneous downgrade of cellulose as well as hemicellulose (Reddy and Rhim 2018). For raw PPF, the third stage of mass loss starts at 360°C and for optimally surface-modified PPF; it is started from 375°C however at 550°C both the fibers were having the same quantity of mass residual (27 wt%). The third stage of mass loss denoted the deterioration of lignin, wax and other oily contents presented in the fiber (Manimaran et al. 2018a). DTG curve confirmed that cellulose degradation temperature of the optimally surfacemodified PPF is enhanced from 332°C to 348°C. Similarly, enhancement of cellulose degradation temperature was noticed in the alkali-treated Prosopis juliflora, Coccinia grandis.L, Acacia planifrons and Acacia leucophloea (Arthanarieswaran, Kumaravel, and Saravanakumar 2015; Madhu et al. 2018b; Senthamaraikannan and Kathiresan 2018; Senthamaraikannan et al. 2016).

Table 3. Tensile properties of untreated and optimally surface modified PPF.

Fiber	Tensile Strength (MPa)	Tensile Modulus (GPa)	Elongation at break (%)	
Raw PPF	322 ± 16.10	9.67 ± 0.144	2.09 ± 0.214	
Optimally treated PPF	343.6 ± 13.04	12.71 ± 0.132	1.98 ± 0.145	

Kinetic activation energy (E_a) measurement is another method of evaluating thermal stability of the bio-fibers (Grønli, Várhegyi, and Di Blasi 2002). The Broido plot of untreated and optimally surface-modified PPF (Figure 4b) was drawn, and Kinetic activation energy of the PPF was measured with the aid of Broido plots and Equation (3) (Broido 1969).

$$\ln\left[\ln\left(\frac{1}{y}\right)\right] = -\left(\frac{E_a}{R}\right)\left[\left(\frac{1}{T}\right) + K\right]$$
(3)

Where, y – Normalized mass of the fibers (m_t/m_o) , m_o .Initial mass of fibers at room temperature, m_t .Mass of the fibers at any temperature, E_a . Kinetic activation energy, R-8.32 kJ/molK (ideal gas constant), T- Temperature (Kelvin) and K – reaction rate constant. The E_a of the optimally treated PPF was improved to 72.563 KJ/mol from 68.642 KJ/mol which was accredited to the conversion of hemicellulose to cellulose, removal of lignin and wax content from the optimally surface-modified PPF (Ganapathy et al. 2019). The E_a of the optimally treated PPF (72.563 KJ/mol) was higher than the *Lygeum spartum* (68.77 kJ/mol), *Furcraea foetida* (65.64 kJ/mol) and lower than the Cissus *quadrangularis* root (74.18 kJ/mol) (Belouadah, Ati, and Rokbi 2015; Manimaran et al.

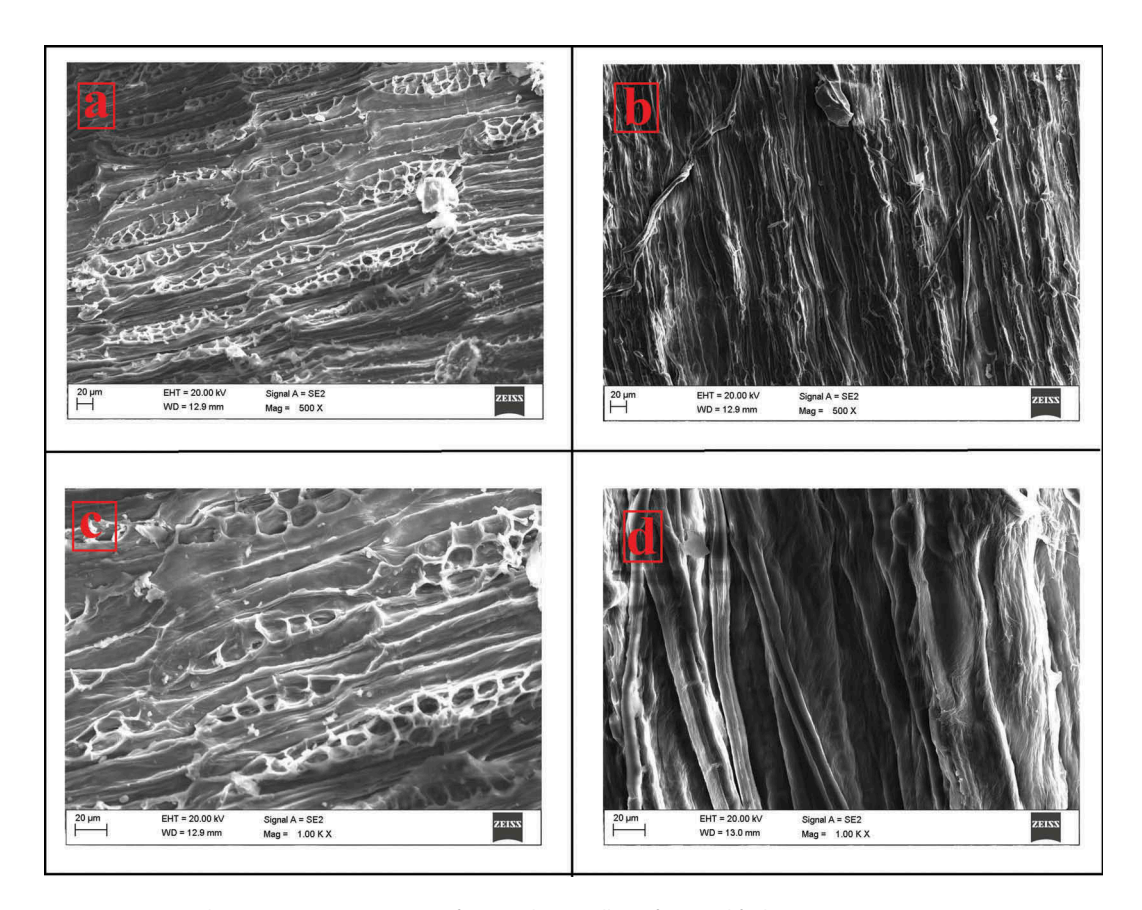


Figure 6. Scanning electron microscopic images of raw and optimally surface modified PPF.



2017). Above findings authenticated that untreated and surface modified PPF are appropriate material to fabricate the fiber reinforced plastics.

Single-fiber tensile test

Tensile properties of raw and optimally surface-modified PPF were tabularized in Table 3. Tensile strength of the optimally surface-modified PPF was boosted from 322 ± 16.10 MPa to 343.6 ± 13.04 MPa, which may be occurred because of enhancement in the amount of cellulose content in the optimally surface-modified PPF. Tensile modulus of the untreated, optimally surface-modified PPF were calculated as 9.67 ± 0.144 GPa and 12.71 ± 0.132 GPa respectively which are quite higher than the other natural fibers such as Sansevieria ehrenbergii (1.5-7.67 GPa), Grewia tilifolia (4.5671 GPa) and Manicaria saccifera palm (2.20 ± 0.44) (Porras, Maranon, and Ashcroft 2015; Sathishkumar et al. 2013). The strain rate of the optimally surface-modified PPF is slightly reduced from $2.09 \pm 0.214\%$ to $1.98 \pm 0.145\%$. The statistical analysis curves (Weibull distribution) of tensile strength and tensile modulus of untreated and optimally surface-modified PPF were displayed in Figure 5. Figure 5 confirmed that tensile strength and modulus of the majority of the raw and optimally surface-modified fibers were located within the line and match absolutely the Weibull distribution (Balaji and Nagarajan 2017).

Surface morphological analyses

Scanning electron microscope

It is significant to analyze the surface morphology of the plant fibers to predict the bonding nature of the fiber with the matrix. Scanning electron micrograms of untreated and optimally surface-modified PPF were presented in Figure 6. Figure 6a exposed that many of the micro-holes and cracks were appeared in the outer layer of the untreated PPF (Mayandi et al. 2016). Figure 6c acknowledged that wax, lignin and other contaminations also existed on the external surface of the untreated PPF. Generally, NaOH treatment dissolves the wax and lignin content on the surface of the plant fibers (Ivanovska et al. 2019). Figure 6b confirmed that elimination of wax, lignin and pollutant in the

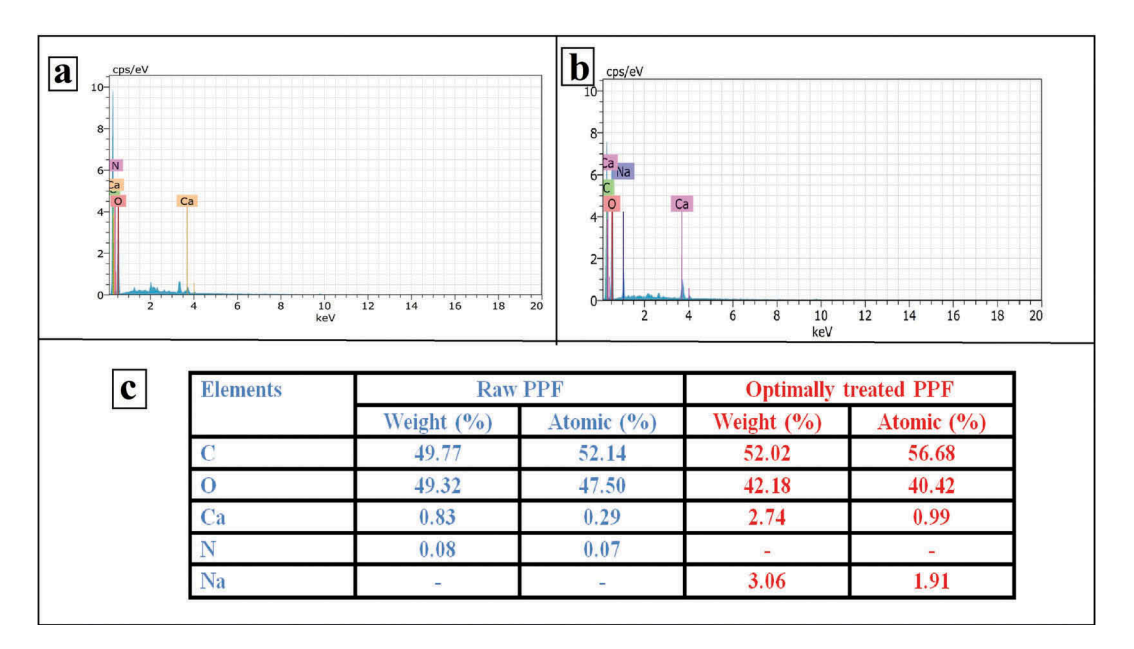


Figure 7. Energy dispersive X-Ray spectroscopic analysis of (a) untreated and (b) optimally surface modified PPF (c) quantity of elements dispersed on the outer layer of untreated and optimally surface modified PPF.

outer layer of the PPF after surface modification. Figure 6d demonstrated that micro-holes and cracks were also disappeared after the NaOH treatment.

Energy-dispersive x-ray spectroscopy

EDX spectrums of raw and optimally surface-modified PPF were exhibited in Figure 7a,b respectively. The quantity of various elements available on the untreated and optimally surface-modified PPF was also demonstrated in Figure 7c. As a plant fiber, both untreated and optimally treated PPF are having a higher quantity of Carbon (C) and Oxygen (O) content than other elements (Manimaran et al. 2017). Nitrogen (N) and Calcium (Ca) content present in the raw PPF evidenced that impurities were present in the untreated PPF. After the alkali treatment, Nitrogen content was removed entirely, and Calcium content was considerably reduced. Sodium (Na) content was visible only on the alkali-treated PPF due to the deposition of sodium during the NaOH treatment (Senthamaraikannan and Kathiresan 2018).

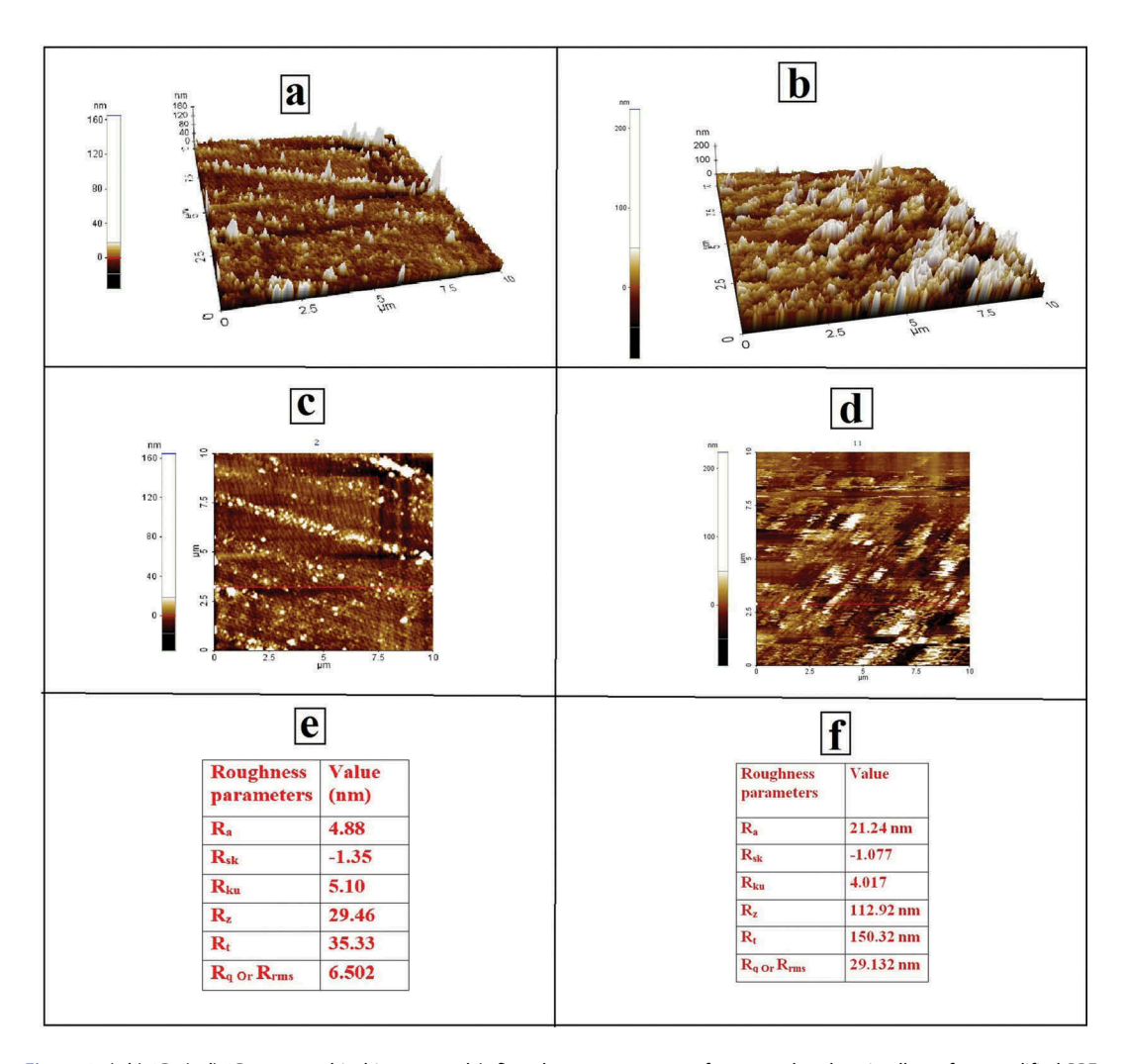


Figure 8. (a,b) 3D, (c,d) 2D topographical images and (e,f) roghness parameters of untreated and optimally surface modified PPF.



Atomic force microscopy

3D, 2D topographical images and surface topographical values of raw, optimally surface-modified PPF were exhibited in Figure 8a-f respectively. 3D, 2D topographical images revealed that optimally surfacemodified PPF has a rougher surface than the untreated PPF. Improved Ra value (21.42 nm) of PPF evidenced the removal of amorphous content (lignin, wax and hemicelluloses) and contaminations on the outer layer of the optimally surface-modified PPF (Manimaran et al. 2017). Negative Rsk values of both untreated and optimally surface-modified PPF were indicated the micropores exiting in the both raw and optimally surface-modified fibers. Reduced Rku values (4.017) of the optimally surfacemodified PPF pointed out the relatively rough surface existing on the fiber (Balasundar et al. 2018). Rt and Rrms values of the optimally surface-modified PPF were also enhanced. All the above modifications in the surface topography of the optimally surface-modified PPF concluded that optimally surfacemodified PPF is a suitable material to make lightweight fiber reinforced plastics.

Conclusion

Chemical compositional analysis outcomes proved that 5% (w/v) NaOH with 60 minutes treated PPF was optimally surface-modified fiber because it produced more positive change in chemical composition than all other soaking time such as 15, 30, 45, 75 minutes. Elimination of lignin content in the fiber was verified through the FTIR analysis. The XRD analysis evidenced improvement in the crystallinity index (CI) (45.31% to 52.43%) and crystallite size (CS) (5.43 nm to 8.32 nm) of the optimally surface-modified PPF. TGA and DTG curves witnessed the improvement (332°C to 348°C) in the cellulose degradation temperature of the optimally surface-modified PPF. Tensile strength and modulus of the optimally surface-modified PPF were increased from 322 ± 16.10 MPa to 343.6 ± 13.04 MPa, 9.67 ± 0.144 GPa to 12.71 ± 0.132 GPa respectively. Surface topography of the optimally surface-modified fiber is positively altered after the alkalization. All the above experimental reports proved that optimally surface-modified PPF were comparatively better reinforcement material for thermoset polymer composite.

References

- Ali, M. 2016. Microstructure, thermal analysis and acoustic characteristics of calotropis procera (Apple of Sodom) fibers. Journal of Natural Fibers 13 (3):343-52. doi:10.1080/15440478.2015.1029198.
- Arthanarieswaran, V. P., A. Kumaravel, and S. S. Saravanakumar. 2015. Physico-chemical properties of alkali-treated acacia leucophloea fibers. International Journal of Polymer Analysis and Characterization 20 (8):704-13. doi:10.1080/1023666X.2015.1081133.
- Atiqah, A., M. Jawaid, M. R. Ishak, and S. M. Sapuan. 2018. Effect of alkali and silane treatments on mechanical and interfacial bonding strength of sugar palm fibers with thermoplastic polyurethane. Journal of Natural Fibers 15 (2):251-61. doi:10.1080/15440478.2017.1325427.
- Balaji, A. N., and K. J. Nagarajan. 2017. Characterization of alkali treated and untreated new cellulosic fiber from saharan aloe vera cactus leaves. Carbohydrate Polymers 174:200-08. doi:10.1016/j.carbpol.2017.06.065.
- Balasundar, P., P. Narayanasamy, P. Senthamaraikannan, S. Senthil, R. Prithivirajan, and T. Ramkumar. 2018. Extraction and characterization of new natural cellulosic chloris barbata fiber. Journal of Natural Fibers 15 (3):436-44. doi:10.1080/15440478.2017.1349015.
- Baskaran, P. G., M. Kathiresan, P. Senthamaraikannan, and S. S. Saravanakumar. 2018. Characterization of new natural cellulosic fiber from the bark of dichrostachys cinerea. Journal of Natural Fibers 15 (1):62-68. doi:10.1080/ 15440478.2017.1304314.
- Belouadah, Z., A. Ati, and M. Rokbi. 2015. Characterization of new natural cellulosic fiber from Lygeum Spartum L. Carbohydrate Polymers 134 (July 2016):429-37. doi:10.1016/j.carbpol.2015.08.024.
- Broido, A. 1969. A simple, sensitive graphical method of treating thermogravimetric analysis data. Journal of Polymer Science Part A-2: Polymer Physics 7 (10):1761-73. doi:10.1002/pol.1969.160071012.
- Ganapathy, T., R. Sathiskumar, P. Senthamaraikannan, S. S. Saravanakumar, and A. Khan. 2019. Characterization of raw and alkali treated new natural cellulosic Fi bres extracted from the aerial roots of banyan tree. International Journal of Biological Macromolecules 138:573-81. doi:10.1016/j.ijbiomac.2019.07.136.
- Grønli, M. G., G. Várhegyi, and C. Di Blasi. 2002. Thermogravimetric analysis and devolatilization kinetics of wood. Industrial and Engineering Chemistry Research 41 (17):4201-08. doi:10.1021/ie0201157.



- Hyness, N. R. J., N. J. Vignesh, P. Senthamaraikannan, S. S. Saravanakumar, and M. R. Sanjay. 2018. Characterization of new natural cellulosic fiber from heteropogon contortus plant. *Journal of Natural Fibers* 15 (1):146–53. doi:10.1080/15440478.2017.1321516.
- Indran, S., and R. Edwin Raj. 2015. Characterization of new natural cellulosic fiber from cissus quadrangularis stem. *Carbohydrate Polymers* 117:392–99. doi:10.1016/j.carbpol.2014.09.072.
- Ivanovska, A., D. Cerovic, S. Maletic, I. Jankovic Castvan, K. Asanovic, and M. Kostic. 2019. Influence of the alkali treatment on the sorption and dielectric properties of Woven Jute Fabric. *Cellulose* 26 (8):5133–46. doi:10.1007/s10570-019-02421-0.
- Jayaramudu, J., B. R. Guduri, and A. Varada Rajulu. 2010. Characterization of new natural cellulosic fabric Grewia Tilifolia. *Carbohydrate Polymers* 79 (4):847–51. doi:10.1016/j.carbpol.2009.10.046.
- KılınÇ, A. Ç., S. Köktaş, M. Atagür, and M. Ö. Seydibeyoglu. 2018a. effect of extraction methods on the properties of althea officinalis l. fibers. Fibers. Journal Of Natural Fibers 15 (3):325–36. doi: 10.1080/15440478.2017.1325813.
- Kılınç, A. Ç., S. Köktaş, Y. Seki, M. Atagür, R. Dalmış, Ü. H. Erdoğan, A. A. Göktaş, and M. Ö. Seydibeyoğlu. 2018b. Extraction and investigation of lightweight and porous natural fiber from conium maculatum as a potential reinforcement for composite materials in transportation. Composites Part B: Engineering 140 (2018):1–8. doi: 10.1016/j.compositesb.2017.11.059.
- Kumar, R., N. R. J. Hynes, P. Senthamaraikannan, S. Saravanakumar, and M. R. Sanjay. 2018. Physicochemical and thermal properties of ceiba pentandra bark fiber. *Journal of Natural Fibers* 15 (6):822–29. doi:10.1080/15440478.2017.1369208.
- Liu, Y., X. Lv, J. Bao, J. Xie, X. Tang, J. Che, Y. Ma, and J. Tong. 2019a. Characterization of silane treated and untreated natural cellulosic fibre from corn stalk waste as potential reinforcement in polymer composites. *Carbohydrate Polymers*. doi:10.1016/j.carbpol.2019.04.088.
- Liu, Y., Y. Ma, J. Yu, J. Zhuang, S. Wu, and J. Tong. 2019b. Development and characterization of alkali treated abaca fiber reinforced friction composites. *Composite Interfaces* 26 (1):67–82. doi:10.1080/09276440.2018.1472456.
- Maache, M., A. Bezazi, S. Amroune, F. Scarpa, and A. Dufresne. 2017. Characterization of a novel natural cellulosic fiber from Juncus Effusus L. *Carbohydrate Polymers* 171:163–72. doi:10.1016/j.carbpol.2017.04.096.
- Madhu, P., M. R. Sanjay, P. Senthamaraikannan, S. Pradeep, S. Siengchin, M. Jawaid, and M. Kathiresan. 2018b. Effect of various chemical treatments of *Prosopis Juliflora* fibers as composite reinforcement: Physicochemical, thermal, mechanical, and morphological properties. *Journal of Natural Fibers* 1–12. doi:10.1080/15440478.2018.1534191.
- Madhu, P., M. R. Sanjay, P. Senthamaraikannan, S. Pradeep, S. S. Saravanakumar, and B. Yogesha. 2018a. A review on synthesis and characterization of commercially available natural fibers: Part-I. *Journal of Natural Fibers* 1–13. doi:10.1080/15440478.2018.1453433.
- Maheswari, C. U., K. O. Reddy, E. Muzenda, M. Shukla, and A. V. Rajulu. 2013. A comparative study of modified and unmodified high-density polyethylene/borassus fiber composites. *International Journal of Polymer Analysis and Characterization* 18 (6):439–50. doi:10.1080/1023666X.2013.814027.
- Manimaran, P., M. Prithiviraj, S. S. Saravanakumar, V. P. Arthanarieswaran, and P. Senthamaraikannan. 2018a. Physicochemical, tensile, and thermal characterization of new natural cellulosic fibers from the stems of sida cordifolia. *Journal of Natural Fibers* 15 (6):860–69. doi:10.1080/15440478.2017.1376301.
- Manimaran, P., M. R. Sanjay, P. Senthamaraikannan, B. Yogesha, C. Barile, and S. Siengchin. 2018b. A new study on characterization of pithecellobium dulce fiber as composite reinforcement for light-weight applications. *Journal of Natural Fibers* 1–12. doi:10.1080/15440478.2018.1492491.
- Manimaran, P., P. Senthamaraikannan, K. Murugananthan, and M. R. Sanjay. 2018c. Physicochemical properties of new cellulosic fibers from azadirachta indica plant. *Journal of Natural Fibers* 15 (1):29–38. doi:10.1080/15440478.2017.1302388.
- Manimaran, P., P. Senthamaraikannan, M. R. Sanjay, M. K. Marichelvam, and M. Jawaid. 2017. Study on characterization of furcraea foetida new natural fiber as composite reinforcement for lightweight applications. Carbohydrate Polymers. doi:10.1016/j.carbpol.2017.11.099.
- Manimaran, P., P. Senthamaraikannan, M. R. Sanjay, M. K. Marichelvam, and M. Jawaid. 2018d. Study on characterization of furcraea foetida new natural fiber as composite reinforcement for lightweight applications. *Carbohydrate Polymers* 181:650–58. doi:10.1016/j.carbpol.2017.11.099.
- Mayandi, K., N. Rajini, P. Pitchipoo, J. T. Winowlin Jappes, and A. Varada Rajulu. 2016. Extraction and characterization of new natural lignocellulosic fiber cyperus pangorei. *International Journal of Polymer Analysis and Characterization* 21 (2):175–83. doi:10.1080/1023666X.2016.1132064.
- Porras, A., A. Maranon, and I. A. Ashcroft. 2015. Characterization of a novel natural cellulose fabric from manicaria saccifera palm as possible reinforcement of composite materials. *Composites Part B: Engineering* 74:66–73. doi:10.1016/j.compositesb.2014.12.033.
- Reddy, J. P., and J. W. Rhim. 2018. Extraction and characterization of cellulose microfibers from agricultural wastes of onion and garlic. *Journal of Natural Fibers* 15 (4):465–73. doi:10.1080/15440478.2014.945227.
- Reddy, K. O., C. U. Maheswari, D. J. P. Reddy, and A. V. Rajulu. 2009. Thermal properties of napier grass fibers. *Materials Letters* 63 (27):2390–92. doi:10.1016/j.matlet.2009.08.035.



- Reddy, K. O., C. U. Maheswari, E. Muzenda, M. Shukla, and A. V. Rajulu. 2016. Extraction and characterization of cellulose from pretreated ficus (Peepal Tree) leaf fibers. *Journal of Natural Fibers* 13 (1):54–64. doi:10.1080/15440478.2014.984055.
- Reddy, K. O., K. R. N. Reddy, J. Zhang, J. Zhang, and A. V. Rajulu. 2013. Effect of alkali treatment on the properties of century fiber. *Journal of Natural Fibers* 10 (3):282–96. doi:10.1080/15440478.2013.800812.
- Rwawiire, S., and B. Tomkova. 2015. Morphological, thermal, and mechanical characterization of sansevieria trifasciata fibers. *Journal of Natural Fibers* 12 (3):201–10. doi:10.1080/15440478.2014.914006.
- Sanjay, M. R., S. Siengchin, J. Parameswaranpillai, M. Jawaid, C. I. Pruncu, and A. Khan. 2019. A comprehensive review of techniques for natural fibers as reinforcement in composites: Preparation, processing and characterization. *Carbohydrate Polymers* 207 (November 2018):108–21. doi:10.1016/j.carbpol.2018.11.083.
- Saravana Kumaar, A., A. Senthilkumar, T. Sornakumar, S. S. Saravanakumar, and V. P. Arthanariesewaran. 2017. Physicochemical properties of new cellulosic fiber extracted from carica papaya bark. *Journal of Natural Fibers* 1–10. doi:10.1080/15440478.2017.1410514.
- Saravanakumar, S. S., A. Kumaravel, T. Nagarajan, and I. Ganesh Moorthy. 2014. Investigation of physico-chemical properties of alkali-treated prosopis juliflora fibers. *International Journal of Polymer Analysis and Characterization* 19 (4):309–17. doi:10.1080/1023666X.2014.902527.
- Sathishkumar, T. P., P. Navaneethakrishnan, S. Shankar, and R. Rajasekar. 2013. Characterization of new cellulose sansevieria ehrenbergii fibers for polymer composites. *Composite Interfaces* 20 (8):575–93. doi:10.1080/15685543.2013.816652.
- Segal, L., J. J. Creely, A. E. Martin, and C. M. Conrad. 1959. An empirical method for estimating the degree of crystallinity of native cellulose using the X-ray diffractometer. *Textile Research Journal* 29 (10):786–94. doi:10.1177/ 004051755902901003.
- Senthamaraikannan, P., and M. Kathiresan. 2018. Characterization of raw and alkali treated new natural cellulosic fiber from Coccinia Grandis.L. *Carbohydrate Polymers* 186:332–43. doi:10.1016/j.carbpol.2018.01.072.
- Senthamaraikannan, P., S. S. Saravanakumar, V. P. Arthanarieswaran, and P. Sugumaran. 2016. Physico-chemical properties of new cellulosic fibers from the bark of acacia planifrons. *International Journal of Polymer Analysis and Characterization* 21 (3):207–13. doi:10.1080/1023666X.2016.1133138.
- Shanmugasundaram, N., I. Rajendran, and T. Ramkumar. 2018. Characterization of untreated and alkali treated new cellulosic fiber from an area palm leaf stalk as potential reinforcement in polymer composites. *Carbohydrate Polymers* 195:566–75. doi:10.1016/j.carbpol.2018.04.127.
- Sreenivasan, V. S., S. Somasundaram, D. Ravindran, V. Manikandan, and R. Narayanasamy. 2011. Microstructural, physico-chemical and mechanical characterisation of sansevieria cylindrica fibres An exploratory investigation. *Materials and Design* 32 (1):453–61. doi:10.1016/j.matdes.2010.06.004.
- Syafri, E., A. Kasim, A. Asben, P. Senthamaraikannan, and M. R. Sanjay. 2018. Studies on ramie cellulose microfibrils reinforced cassava starch composite: Influence of microfibrils loading. *Journal of Natural Fibers* 1–10. doi:10.1080/15440478.2018.1470057.
- Thakur, V. K., and M. K. Thakur. 2014. Processing and characterization of natural cellulose fibers/thermoset polymer composites. *Carbohydrate Polymers* 109:102–17. doi:10.1016/j.carbpol.2014.03.039.
- Umashankaran., M., and S. Gopalakrishnan. 2019. Characterization of bio-fiber from Pongamiapinnata L. bark as possible reinforcement of polymer composites. *Journal of Natural Fibers* 1–11. doi:10.1080/15440478.2019.1658254.